




ORIGINAL RESEARCH

Dual-user joint sensing and communications with time-divisioned bi-static radar

Enhao Wang  | Yunfei Chen  | Aissa Ikhlef | Hongjian Sun 

Department of Engineering, Durham University,
Durham, UK

Correspondence

Yunfei Chen, Department of Engineering, Durham
University, Durham, UK.
Email: Yunfei.Chen@durham.ac.uk

Funding information

HORIZON EUROPE MSCA-SE, Grant/Award
Number: 101129618 UNITE; Engineering and
Physical Sciences Research Council, Grant/Award
Numbers: EP/Y036581/1, EP/Y037243/1,
EP/X04047X/1

Abstract

Joint sensing and communications systems have gained significant research interest by merging sensing capabilities with communication functionalities. However, few works have examined the case of multiple users. This work investigates a dual-user joint sensing and communications system, focusing on the interference between the users that explores the optimal performance trade-offs through a time-division approach. Bi-static radar setting is considered. Two typical strategies under this approach are studied: one in which both users follow the same order of communications and then sensing, and the other in which the tasks are performed in opposite order at two users. In each strategy, the sum rate and the detection probability are evaluated and optimized. The results show that the opposite order strategy offers superior performance to the same order strategy, and they also quantify their performance difference. This research highlights the potential benefits of time-division strategies and multiple users in joint sensing and communications systems.

1 | INTRODUCTION

The development of the sixth-generation (6G) wireless communications systems necessitates both high-data-rate communications and high-precision sensing/localization capabilities [1]. Historically, sensing and communications have been considered as separate functionalities. This separation has led to several issues, such as spectrum congestion and mutual interference. To address these issues, an increasing number of studies are focusing on the combination of communications and sensing technologies [2]. As a key technology to enable this, joint sensing and communications (JSAC) has recently gained momentum [3, 4]. Many of these studies predominantly focus on three key areas: coexistence, cooperation and joint design. Within the field of coexistence, the individual performance metrics of either sensing or communications functions have been evaluated with interference from the other system. For example, in [5–7], the interference between sensing and communications operating in a non-cooperative manner was studied. In the cooperation literature, sensing and communications share information to improve their own performances. For example, sensing and communications performances were optimized by setting constraints on communications and sensing, respectively, in [8–10].

Finally, for joint design, complete cooperation between sensing and communications is adopted by co-designing radar and communications. In many applications, both sensing and communications functions are required in a single system. The joint design of sensing and communications can reduce the cost and energy consumption, as well as alleviate spectrum congestion problems. Furthermore, precise location information of mobile terminals can enhance wireless communication performance and the advancement of communication technologies also presents new opportunities to improve the localization performance greatly [11]. Thus, our focus is on joint design for JSAC.

Unlike mono-static settings used in most previous works on JSAC, in our work, bi-static radar setting is considered. Bi-static setting can help JSAC system achieve better performances [12]. Firstly, positioning the sensing transmitter and receiver separately offers enhanced flexibility and an extended detection range [13]. Secondly, it eliminates the issue of self-interference (SI) in a mono-static setting [14]. Also, many works on JSAC have focused on dual-functional waveform designs, where sensing and communications use the same waveform [15, 16]. However, these schemes often require complicated designs. Reference [17] provided methods for analysing

This is an open access article under the terms of the [Creative Commons Attribution](https://creativecommons.org/licenses/by/4.0/) License, which permits use, distribution and reproduction in any medium, provided the original work is properly cited.

© 2024 The Author(s). *IET Communications* published by John Wiley & Sons Ltd on behalf of The Institution of Engineering and Technology.

sensing performance using generalized likelihood ratio test (GLRT) detectors. The approximations to the distribution of GLRT's decision variable by using moment-matching were proposed in [18]. The JSAC systems typically encounter unavoidable performance tradeoff, which have been thoroughly examined in various studies [4, 5, 7–13]. The performance measures were derived for sensing, communications and JSAC in [19]. The work in [20] focused on the performance trade-off between sensing and communications. Three optimization strategies, time-division, power-allocation, and mixture, were proposed in [21]. The performance trade-off for a time-division scheme where sensing was performed after data communications in the same time frame was analysed in [22].

Most of the above works have only considered a single user. In communications systems, multiple users are often present, causing interference to each other. This interference could degrade communications but could also improve sensing due to extra reflection. Therefore, it is of great interest to study JSAC with bi-static radar in the presence of multiple users. Multiple users have been considered in some applications. For example, reference [23] proposed a multi-user uplink communication scheme against a mobile aerial eavesdropper (AE) in JSAC systems, where the JSAC base station (BS) transmits radar signals to track and jam the AE. Reference [24] proposed a symbol-level precoding (SLP) method for a multi-user multi-input multi-output (MU-MIMO) downlink JSAC system based on faster-than-Nyquist (FTN) signalling. However, none of these works has considered time-division or bi-static setting.

Motivated by the above observations, in this work, a dual-user JSAC system using time-divisioned bi-static radar is studied, where two users adopt the same or different time allocation strategies, unlike [17–22] that only considered a single JSAC user without any interference from other users, or [23] and [24] without time division or bi-static setting. One challenge addressed in this work is the extension from a single user in [17–22] to two users. This is difficult, because the extra user induces interference into the system so that the sensing and communications tasks need to adapt to the interfering power and the tasks of one user affect the performance of the other user. For the case of more than two users, users can be paired up as groups of two for study, similar to the work on non-orthogonal multiple access [25]. Another challenge addressed in this work is the use of bi-static setting and time division between sensing and communications. Bi-static setting often has weaker received signals than mono-static setting, making their target detection more difficult due to high sensitivity and synchronization requirements. Time division requires even higher synchronization between users and between tasks. Communications-centric, sensing-centric and joint designs are considered. All three designs are optimized with respect to the time allocation parameters. Numerical results show that the system performance can be improved when the two users perform different functions at the same time. The main contributions of this work can be summarized as follows:

- This work considers interference and cooperation between two JSAC users with bi-static setting, while most previous works only studied a single JSAC user.

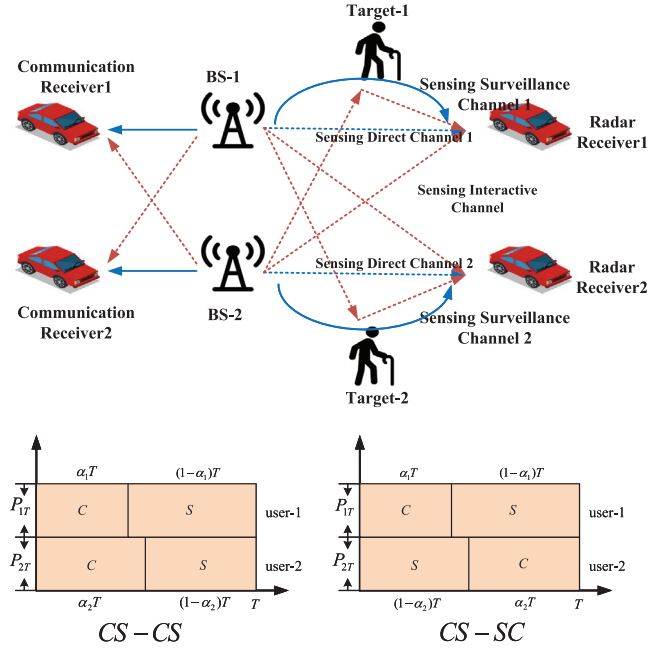


FIGURE 1 Joint sensing and communications system using bi-static radar.

- For the dual-user case, two time allocation strategies when the two users either perform communications and sensing in the same order or in the opposite order are studied. For each strategy, three optimization problems are formulated and solved by guaranteeing a minimum requirement on sensing, on communications or no requirement.

The rest of the article is organized as follows. In Section 2, the system model and the two strategies will be presented. In Section 3, the performance tradeoff between communications and sensing and their optimization will be formulated and solved. In Section 4, numerical results will be presented. Finally, in Section 5, concluding remarks will be made.

2 | SYSTEM MODEL

Consider a dual-user JSAC system, where each user operates with a separate JSAC scheme in time-division and bi-static settings, as illustrated in Figure 1. Each JSAC user consists of one BS as transmitter, one target to detect, one sensing receiver and one communications receiver, similar to the models used in [17–22]. In order to focus on the interference between different JSAC users, assume that the sensing and communications functions at each user adopt different frequencies to avoid the interference between different functions and that the BS cannot operate at two frequencies or two functions at the same time.

Without loss of generality, assume that the total transmission time of each user is fixed at T seconds and that the total transmission power of user- x is P_{xT} for both radar and communications, where $x = 1$ for user-1 and $x = 2$ for user-2. Moreover, assume that the transmission time and the

transmission power for sensing, the transmission time and the transmission power for communications of user- x are T_{xr} , P_{xr} , T_{xc} , P_{xc} , respectively. Let T_s be the sampling interval.

2.1 | CS-CS

In the communication-sensing and communication-sensing (CS-CS) strategy, two independent JSAC users perform communications and sensing tasks in the same order, that is, communications first and then sensing within a fixed amount of time T seconds. Hence, one has $T_{1c} + T_{1r} = T$, $T_{2c} + T_{2r} = T$, $P_{1c} = P_{1r} = P_{1T}$, and $P_{2c} = P_{2r} = P_{2T}$. Depending on the length of time allocated to the communications function, the received signals at the communications receivers have two different cases:

2.1.1 | $T_{1c} \geq T_{2c}$

In this case, the communication time of user-1 is longer than that of user-2. Since communications and sensing operate at different frequencies, there is no interference between communications and sensing but there is still interference between communications by different users, as they operate at the same frequency. The received signals at the two communications receivers for two users are given by

$$\mathbf{y}_{1c} = \sqrt{P_{1T}}b_{11c}\mathbf{w}_{1c} + \sqrt{P_{2T}}b_{21c}\mathbf{w}_{2c} + \mathbf{n}_{1c} \quad (1)$$

$$\mathbf{y}_{2c} = \sqrt{P_{2T}}b_{22c}\mathbf{w}_{2c} + \sqrt{P_{1T}}b_{12c}\mathbf{w}_{1cm} + \mathbf{n}_{2c} \quad (2)$$

where $\mathbf{y}_{1c} = [y_{1c1}, \dots, y_{1cK_1}]^T$, $\mathbf{y}_{2c} = [y_{2c1}, \dots, y_{2cK_2}]^T$, $\mathbf{w}_{1c} = [w_{1c1}, w_{1c2}, \dots, w_{1cK_1}]^T$, $\mathbf{w}_{2c} = [w_{2c1}, \dots, w_{2cK_2}]^T$, $\mathbf{w}_{1cm} = [w_{1cm1}, \dots, w_{1cmK_2}]^T$, $K_1 = \frac{T_{1c}}{T_s}$ and $K_2 = \frac{T_{2c}}{T_s}$ represent the total numbers of samples for communications at two users, $K_1 > K_2$, $\sqrt{P_{1T}}$ and $\sqrt{P_{2T}}$ represent the transmitting amplitudes of two users, b_{11c} and b_{22c} are the complex channel coefficients from user-1 and user-2's transmitters to their own communications receivers, b_{12c} and b_{21c} are the complex cross-channel coefficients from user-1's and user-2's transmitters to the other users' communications receivers, w_{1ci} and w_{2ci} are signals transmitted by the two users, w_{1cm} and w_{1ci} only differ in their subscripts. If constant modulus modulation schemes, such as phase shift keying (PSK), are used, the transmitted signals satisfy $|w_{1ci}|^2 = |w_{2ci}|^2 = 1$, where $i = 1, 2, \dots, K_1$ or K_2 . It is known that constant modulus modulation is beneficial to radar detection [26]. Note that, \mathbf{w}_{1cm} is a part of \mathbf{w}_{1c} containing its first K_2 elements, $\mathbf{n}_{jc} = [n_{jc1}, n_{jc2}, \dots, n_{jcK_j}]^T$ is $K_j \times 1$ vector, $j = 1, 2$ and $[\cdot]^T$ represents the transpose operation, n_{1ci} and n_{2ci} are the complex additive white Gaussian noise (AWGN) with mean zero and variance σ^2 , assuming that two users use the same receivers. It is assumed that the noise samples are independent of each other so that the covariance matrices of \mathbf{n}_{1c} and \mathbf{n}_{2c} are given by $\sigma^2\mathbf{I}_{K_1}$ and $\sigma^2\mathbf{I}_{K_2}$ respectively, where \mathbf{I}_{K_1}

and \mathbf{I}_{K_2} are the identity matrix but with different dimensions of K_1 and K_2 , respectively.

From Equations (1) and (2), when $0 < t \leq T_{2c}$, both users are performing communications tasks and their transmitted signals will interfere with each other. When $T_{2c} < t \leq T_{1c}$, user-2 stops transmitting communications signals. During this period, user-1 continues with its communications function. In this case, user-1 only suffers from noise.

Using the signals in Equations (1) and (2), the information rates in bits/Hz for the two communications users can be derived as

$$C_1 = T_{2c} \log_2 \left(1 + \frac{P_{1T}\gamma_{11c}}{P_{2T}\gamma_{21c} + 1} \right) + (T_{1c} - T_{2c}) \log_2 (1 + P_{1T}\gamma_{11c}) \quad (3)$$

$$C_2 = T_{2c} \log_2 \left(1 + \frac{P_{2T}\gamma_{22c}}{P_{1T}\gamma_{12c} + 1} \right) \quad (4)$$

where $\gamma_{11c} = \frac{|b_{11c}|^2}{\sigma^2}$ and $\gamma_{22c} = \frac{|b_{22c}|^2}{\sigma^2}$ are signal-to-noise ratios (SNRs) in the channel from user-1's and user-2's transmitters to their own communications receivers, $\gamma_{12c} = \frac{|b_{12c}|^2}{\sigma^2}$ and $\gamma_{21c} = \frac{|b_{21c}|^2}{\sigma^2}$ are signal-to-noise ratio in the channel from user-1 to user-2 or vice versa. For user- x , $\delta_x = \frac{P_{xT}\gamma_{xxc}}{P_{yT}\gamma_{yxc} + 1}$ represents its signal to interference plus noise ratio (SINR) at its communications receiver, where $x = 1, y = 2$ or $x = 2, y = 1$.

Therefore, the sum rate of the two users in bits/Hz in this case can be derived as

$$\begin{aligned} C &= C_1 + C_2 \\ &= T_{2c} \log_2 \left(1 + \frac{P_{1T}\gamma_{11c}}{P_{2T}\gamma_{21c} + 1} \right) \\ &\quad + T_{2c} \log_2 \left(1 + \frac{P_{2T}\gamma_{22c}}{P_{1T}\gamma_{12c} + 1} \right) \\ &\quad + (T_{1c} - T_{2c}) \log_2 (1 + P_{1T}\gamma_{11c}). \end{aligned} \quad (5)$$

In the CS-CS strategy, after communications, sensing is performed. Specifically, the sensing detection can be formulated as a binary hypothesis testing problem [21]. However, the model becomes more complex due to the user interference. There is a cross channel between the two users, allowing each user to utilize the signal from the other user to help sensing. In particular, the hypothesis test for user-1 is

H_0 :

$$\begin{cases} \mathbf{y}_{1d} = \sqrt{P_{1T}}b_{11d}\mathbf{w}_{1r} + \sqrt{P_{2T}}b_{21d}\mathbf{w}_{2rn} + \mathbf{n}_{1d} \\ \mathbf{y}_{1s} = \mathbf{n}_{1s} \end{cases} \quad (6)$$

H_1 :

$$\begin{cases} \mathbf{y}_{1d} = \sqrt{P_{1T}}b_{11d}\mathbf{w}_{1r} + \sqrt{P_{2T}}b_{21d}\mathbf{w}_{2rn} + \mathbf{n}_{1d} \\ \mathbf{y}_{1s} = \sqrt{P_{1T}}b_{11s}\mathbf{w}_{1r} + \sqrt{P_{2T}}b_{21s}\mathbf{w}_{2rn} + \mathbf{n}_{1s} \end{cases} \quad (7)$$

and the hypothesis test for user-2 is

$H_0 :$

$$\begin{cases} \mathbf{y}_{2d} = \sqrt{P_{2T}}b_{22d}\mathbf{w}_{2r} + \sqrt{P_{1T}}b_{12d}\mathbf{w}_{1r} + \mathbf{n}_{2d} \\ \mathbf{y}_{2s} = \mathbf{n}_{2s} \end{cases} \quad (8)$$

$H_1 :$

$$\begin{cases} \mathbf{y}_{2d} = \sqrt{P_{1T}}b_{22d}\mathbf{w}_{2r} + \sqrt{P_{1T}}b_{12d}\mathbf{w}_{1r} + \mathbf{n}_{2d} \\ \mathbf{y}_{2s} = \sqrt{P_{2T}}b_{22s}\mathbf{w}_{2r} + \sqrt{P_{1T}}b_{12s}\mathbf{w}_{1r} + \mathbf{n}_{2s} \end{cases} \quad (9)$$

where $\mathbf{y}_{1d} = [y_{1d1}, \dots, y_{1dL_1}]^T$, $\mathbf{y}_{1s} = [y_{1s1}, \dots, y_{1sL_1}]^T$, $\mathbf{y}_{2d} = [y_{2d1}, \dots, y_{2dL_2}]^T$, $\mathbf{y}_{2s} = [y_{2s1}, \dots, y_{2sL_2}]^T$, $\mathbf{w}_{1r} = [w_{1r1}, \dots, w_{1rL_1}]^T$, $\mathbf{w}_{2r} = [w_{2r1}, \dots, w_{2rL_2}]^T$, $\mathbf{w}_{2rn} = [w_{2r(L_2-L_1)}, \dots, w_{2rL_2}]^T$, $\mathbf{n}_{1d} = [\mathbf{n}_{11}, \dots, \mathbf{n}_{1L_1}]^T$, $\mathbf{n}_{2d} = [\mathbf{n}_{21}, \dots, \mathbf{n}_{2L_2}]^T$, \mathbf{y}_{1d} and \mathbf{y}_{2d} are the signals in the direct channels, \mathbf{y}_{1s} and \mathbf{y}_{2s} are the signals in the surveillance channels, $L_1 = \frac{T_{1r}}{T_s}$ and $L_2 = \frac{T_{2r}}{T_s}$ represent the total numbers of samples for communications at two users, $L_1 < L_2$, b_{11d} and b_{22d} are the complex channel coefficients from user-1's and user-2's transmitters to their own sensing receivers in the direct channels, b_{12d} and b_{21d} are the cross-channel coefficients from user-1's and user-2's transmitters to each other's sensing receivers in the direct channels, b_{11s} and b_{22s} are the channel coefficients from user-1's and user-2's transmitters to their own sensing receiver reflected by the target in the surveillance channels, b_{12s} and b_{21s} are the channel coefficients from user-1's and user-2's transmitters to each other's sensing receivers via the targets in the surveillance channels, w_{1ri} and w_{2rj} are the transmitted signals for sensing detection, n_{1di} , n_{1si} , n_{2dj} , and n_{2sj} are the complex AWGN with mean zero and variance σ^2 , $i = 1, \dots, L_1$ and $j = 1, \dots, L_2$.

Similarly, we set $|w_{1ri}|^2 = 1$ and $|w_{2rj}|^2 = 1$ with constant modulus, leading to $\mathbf{w}_{1r}^H \mathbf{w}_{1r} = L_1$ and $\mathbf{w}_{2r}^H \mathbf{w}_{2r} = L_2$, where $(\cdot)^H$ is the Hermitian operation. For example, this is the case when linear frequency modulation is utilized for radar sensing. Again, assume that the noise samples are independent with the covariance matrices of \mathbf{n}_{1d} , \mathbf{n}_{1s} , \mathbf{n}_{2d} , and \mathbf{n}_{2s} being given by $\sigma^2 \mathbf{I}_{L_1}$ or $\sigma^2 \mathbf{I}_{L_2}$. It is also assumed that clutters have already been included in the noise in Equations (6)–(9), similar to [17–22]. Note that both \mathbf{w}_{xr} and \mathbf{w}_{xr} are assumed unknown but deterministic. The coefficients of the radar channels b_{xyd} and b_{xys} are not known either for $x, y = 1, 2$. In this case, the GLRT detector can be used. Details of this detector can be found in [17]. Using this detector, if $\gamma_{xyd} = \frac{|b_{xyd}|^2}{\sigma^2}$, the probability of false alarm can be approximated as [21]

$$FA \approx e^{-\lambda} \quad (10)$$

where λ is the detection threshold used in the GLRT detector. The probabilities of detection can be approximated as [21]

$$\begin{aligned} DP_1 &\approx \mathcal{Q}_1 \left(\sqrt{2P_{1T}\gamma_{11s} + 2P_{2T}\gamma_{21s}} \sqrt{L_1}, \sqrt{2\lambda} \right) \\ &= \mathcal{Q}_1 \left(\sqrt{2(P_{1T}\gamma_{11s} + P_{2T}\gamma_{21s})L_1}, b \right) \end{aligned} \quad (11)$$

$$\begin{aligned} DP_2 &\approx \mathcal{Q}_1 \left(\sqrt{2P_{2T}\gamma_{22s} + 2P_{1T}\gamma_{12s}} \sqrt{L_2}, \sqrt{2\lambda} \right) \\ &= \mathcal{Q}_1 \left(\sqrt{2P_{1T}\gamma_{22s}L_1 + 2P_{2T}\gamma_{12s}L_2}, b \right) \end{aligned} \quad (12)$$

where $\gamma_{xys} = \frac{|b_{xys}|^2}{\sigma^2}$ is the SNR of the surveillance channel from the transmitter of user- x to the radar receiver of user- y reflected by the target, $b = \sqrt{2\lambda} = \sqrt{-2 \ln(\text{FA})}$ is a constant from Equation (10), FA is the predetermined probability of false alarm, and $\mathcal{Q}_1(\cdot, \cdot)$ is the first-order Marcum Q function [27]. Note that, since $T = T_c + T_r$, one has $N = K_1 + L_1 = K_2 + L_2$, where $N = \frac{T}{T_s}$.

2.1.2 | $T_{1c} < T_{2c}$

In this case, the communications time of user-2 is longer than that of user-1. The received signals are very similar to those in the previous subsection except that the indexes 1 and 2 are swapped. When $0 < t \leq T_{2c}$, the received signals at the communications receivers can be given by

$$\mathbf{y}_{1c} = \sqrt{P_T}b_{11c}\mathbf{w}_{1c} + \sqrt{P_T}b_{21c}\mathbf{w}_{2m} + \mathbf{n}_{1c} \quad (13)$$

$$\mathbf{y}_{2c} = \sqrt{P_T}b_{22c}\mathbf{w}_{2c} + \sqrt{P_T}b_{12c}\mathbf{w}_{1c} + \mathbf{n}_{2c} \quad (14)$$

where $\|\mathbf{w}_{1c}\| = \|\mathbf{n}_{1c}\| = K_1$, $\|\mathbf{w}_{2m}\| = K_2 - K_1$, $\|\mathbf{w}_{2c}\| = \|\mathbf{n}_{2c}\| = K_2$. $\|\cdot\|$ represents the length of the vector. Using Equations (13) and (14), the information rates can be derived as

$$C_1 = T_{1c} \log_2 \left(1 + \frac{P_{1T}\gamma_{11c}}{P_{2T}\gamma_{21c} + 1} \right) \quad (15)$$

$$\begin{aligned} C_2 &= T_{1c} \log_2 \left(1 + \frac{P_{2T}\gamma_{22c}}{P_{1T}\gamma_{12c} + 1} \right) \\ &\quad + (T_{2c} - T_{1c}) \log_2 (1 + P_{2T}\gamma_{22c}) \end{aligned} \quad (16)$$

and the sum rate of the two users can be derived as:

$$\begin{aligned} C &= C_1 + C_2 = T_{1c} \log_2 \left(1 + \frac{P_{1T}\gamma_{11c}}{P_{2T}\gamma_{21c} + 1} \right) \\ &\quad + T_{1c} \log_2 \left(1 + \frac{P_{2T}\gamma_{22c}}{P_{1T}\gamma_{12c} + 1} \right) \\ &\quad + (T_{2c} - T_{1c}) \log_2 (1 + P_{2T}\gamma_{22c}) \end{aligned} \quad (17)$$

For sensing, similar to before, the hypothesis test for user-1 can be written as

$H_0 :$

$$\begin{cases} \mathbf{y}_{1d} = \sqrt{P_{1T}}b_{11d}\mathbf{w}_{1r} + \sqrt{P_{2T}}b_{21d}\mathbf{w}_{2r} + \mathbf{n}_{1d} \\ \mathbf{y}_{1s} = \mathbf{n}_{1s} \end{cases} \quad (18)$$

$H_1 :$

$$\begin{cases} \mathbf{y}_{1d} = \sqrt{P_{1T}}b_{11d}\mathbf{w}_{1r} + \sqrt{P_{2T}}b_{21d}\mathbf{w}_{2r} + \mathbf{n}_{1d} \\ \mathbf{y}_{1s} = \sqrt{P_{1T}}b_{11s}\mathbf{w}_{1r} + \sqrt{P_{2T}}b_{21s}\mathbf{w}_{2r} + \mathbf{n}_{1s} \end{cases} \quad (19)$$

and the hypothesis test for user-2 can be written as

$H_0 :$

$$\begin{cases} \mathbf{y}_{2d} = \sqrt{P_{2T}}b_{22d}\mathbf{w}_{2r} + \sqrt{P_{1T}}b_{12d}\mathbf{w}_{1rn} + \mathbf{n}_{2d} \\ \mathbf{y}_{2s} = \mathbf{n}_{2s} \end{cases} \quad (20)$$

$H_1 :$

$$\begin{cases} \mathbf{y}_{2d} = \sqrt{P_{1T}}b_{22d}\mathbf{w}_{2r} + \sqrt{P_{1T}}b_{12d}\mathbf{w}_{1rn} + \mathbf{n}_{2d} \\ \mathbf{y}_{2s} = \sqrt{P_{2T}}b_{22s}\mathbf{w}_{2r} + \sqrt{P_{1T}}b_{12s}\mathbf{w}_{1rn} + \mathbf{n}_{2s} \end{cases} \quad (21)$$

where $\|\mathbf{w}_{1r}\| = \|\mathbf{n}_{1d}\| = \|\mathbf{n}_{1s}\| = L_1$, $\|\mathbf{w}_{1rn}\| = L_1 - L_2$, $\|\mathbf{w}_{2r}\| = \|\mathbf{n}_{2d}\| = \|\mathbf{n}_{2s}\| = L_2$, w_{1rn} is a part of w_{1r} and $\|\cdot\|$ represent the length of the vector. The detection probabilities become

$$DP_1 \approx \mathcal{Q}_1\left(\sqrt{2P_{1T}\gamma_{11s}\mathbf{w}_{1r}^H\mathbf{w}_{1r} + 2P_{2T}\gamma_{21s}\mathbf{w}_{2r}^H\mathbf{w}_{2r}}, b\right) \quad (22)$$

$$= \mathcal{Q}_1\left(\sqrt{2P_{1T}\gamma_{11s}L_1 + 2P_{2T}\gamma_{21s}L_2}, b\right)$$

$$DP_2 \approx \mathcal{Q}_1\left(\sqrt{2P_{2T}\gamma_{22s}\mathbf{w}_{2r}^H\mathbf{w}_{2r} + 2P_{1T}\gamma_{12s}\mathbf{w}_{1rn}^H\mathbf{w}_{1rn}}, b\right) \quad (23)$$

$$= \mathcal{Q}_1\left(\sqrt{2(P_{1T}\gamma_{12s} + P_{2T}\gamma_{22s})L_2}, b\right)$$

which is similar to that when $T_{1c} > T_{2c}$, expect that indexes 1 and 2 are swapped.

2.2 | CS-SC

In the communication-sensing and sensing-communication (CS-SC) strategy, two users perform sensing and communication functions in the opposite order. Without loss of generality, assume that user-1 performs the communications function first and then performs sensing detection, while user-2 does the opposite.

2.2.1 | $T_{1c} + T_{2c} \geq T$

In the case when $T_{1c} + T_{2c} > T$, the communications times of the two users overlap, which will cause interference. The sensing time does not overlap so there is no cross-channel between them. In this case, the received signals at the communications receivers are given by

$$\mathbf{y}_{1c} = \sqrt{P_{1T}}b_{11c}\mathbf{w}_{1c} + \sqrt{P_{2T}}b_{21c}\mathbf{w}_{2cm} + \mathbf{n}_{1c} \quad (24)$$

$$\mathbf{y}_{2c} = \sqrt{P_{2T}}b_{22c}\mathbf{w}_{2c} + \sqrt{P_{1T}}b_{12c}\mathbf{w}_{1cn} + \mathbf{n}_{2c} \quad (25)$$

where $\mathbf{y}_{1c} = [y_{1c1}, \dots, y_{1cK_1}]^T$, $\mathbf{y}_{2c} = [y_{2c1}, \dots, y_{2cK_2}]^T$, $\mathbf{w}_{1c} = [w_{1c1}, w_{1c2}, \dots, w_{1cK_1}]^T$, $\mathbf{w}_{2c} = [w_{2c1}, \dots, w_{2cK_2}]^T$, $\mathbf{w}_{2cm} = [w_{2c1}, \dots, w_{2c(K_1+K_2-N)}]^T$, $\mathbf{w}_{1cn} = [w_{2cL_2}, \dots, w_{2cK_1}]^T$. Note that, \mathbf{w}_{2cm} is a part of \mathbf{w}_{2c} containing its first $K_1 + K_2 - N$ elements and \mathbf{w}_{1cn} is a part of \mathbf{w}_{1c} containing its last $K_1 + K_2 - N$ elements. $\mathbf{n}_{1c} = [n_{1c1}, n_{1c2}, \dots, n_{1cK_1}]^T$ and $\mathbf{n}_{2c} = [n_{2c1}, n_{2c2}, \dots, n_{2cK_2}]^T$ are vectors, and all other symbols are defined as before.

Following the same method in Section 2.1, using Equations (24) and (25), the sum rate of the two users can be derived as

$$\begin{aligned} C &= (T - T_{1c}) \log_2(1 + P_{1T}\gamma_{11c}) \\ &\quad + (T - T_{1c}) \log_2(1 + P_{2T}\gamma_{22c}) \\ &\quad + (T_{1c} + T_{2c} - T_s) \log_2\left(1 + \frac{P_{1T}\gamma_{11c}}{P_{2T}\gamma_{21c} + 1}\right) \\ &\quad + (T_{1c} + T_{2c} - T_s) \log_2\left(1 + \frac{P_{2T}\gamma_{22c}}{P_{1T}\gamma_{12c} + 1}\right). \end{aligned} \quad (26)$$

Similarly, the hypothesis tests for user-1 and user-2 are

$$H_0 : \begin{cases} \mathbf{y}_{1d} = \sqrt{P_{1T}}b_{11d}\mathbf{w}_{1r} + \mathbf{n}_{1d} \\ \mathbf{y}_{1s} = \mathbf{n}_{1s} \end{cases} \quad (27)$$

$$H_1 : \begin{cases} \mathbf{y}_{1d} = \sqrt{P_{1T}}b_{11d}\mathbf{w}_{1r} + \mathbf{n}_{1d} \\ \mathbf{y}_{1s} = \sqrt{P_{1T}}b_{11s}\mathbf{w}_{1r} + \mathbf{n}_{1s} \end{cases} \quad (28)$$

$$H_0 : \begin{cases} \mathbf{y}_{2d} = \sqrt{P_{2T}}b_{22d}\mathbf{w}_{2r} + \mathbf{n}_{2d} \\ \mathbf{y}_{2s} = \mathbf{n}_{2s} \end{cases} \quad (29)$$

$$H_1 : \begin{cases} \mathbf{y}_{2d} = \sqrt{P_{1T}}b_{22d}\mathbf{w}_{2r} + \mathbf{n}_{2d} \\ \mathbf{y}_{2s} = \sqrt{P_{2T}}b_{22s}\mathbf{w}_{2r} + \mathbf{n}_{2s} \end{cases} \quad (30)$$

where $\|\mathbf{w}_{1r}\| = \|\mathbf{n}_{1d}\| = \|\mathbf{n}_{1s}\| = L_1$, $\|\mathbf{w}_{2r}\| = \|\mathbf{n}_{2d}\| = \|\mathbf{n}_{2s}\| = L_2$, $\|\cdot\|$ represent the length of the vector. The sensing detection probabilities of the two users are

$$DP_1 \approx \mathcal{Q}_1\left(\sqrt{2P_{1T}\gamma_{11s}\mathbf{w}_{1r}^H\mathbf{w}_{1r}}, b\right) \quad (31)$$

$$= \mathcal{Q}_1\left(\sqrt{2P_{1T}\gamma_{11s}L_1}, b\right)$$

$$DP_2 \approx \mathcal{Q}_1\left(\sqrt{2P_{2T}\gamma_{22s}\mathbf{w}_{2r}^H\mathbf{w}_{2r}}, b\right) \quad (32)$$

$$= \mathcal{Q}_1\left(\sqrt{2P_{2T}\gamma_{22s}L_2}, b\right).$$

It can be seen that the detection probabilities in this case is similar to the single user case in [21], as they do not overlap with each other.

2.2.2 | $T_{1c} + T_{2c} < T$

In the case when $T_{1c} + T_{2c} < T$, the communications times of the two users do not overlap, so there is no interference. This is based on our assumption that sensing and communications operate at different frequencies. In this case, user 1 will finish their communications before user 2 starts their communications. Since the two communications do not happen at the same time, there is no interference between them. However, the sensing times overlap which leads to a cross-channel and therefore cooperation between the two users. In this case, the received signals at the communications receivers are given by

$$\mathbf{y}_{1c} = \sqrt{P_{1T}} b_{11c} \mathbf{w}_{1c} + \mathbf{n}_{1c} \quad (33)$$

$$\mathbf{y}_{2c} = \sqrt{P_{2T}} b_{22c} \mathbf{w}_{2c} + \mathbf{n}_{2c} \quad (34)$$

and the sum rate for two users are

$$C = T_{1c} \log_2 (1 + P_{1T} \gamma_{11c}) + T_{2c} \log_2 (1 + P_{2T} \gamma_{22c}). \quad (35)$$

Similarly, the hypothesis tests for user-1 and user-2 are

$$H_0 : \begin{cases} \mathbf{y}_{1d} = \sqrt{P_{1T}} b_{11d} \mathbf{w}_{1r} + \sqrt{P_{2T}} b_{21d} \mathbf{w}_{2rn} + \mathbf{n}_{1d} \\ \mathbf{y}_{1s} = \mathbf{n}_{1s} \end{cases} \quad (36)$$

$$H_1 : \begin{cases} \mathbf{y}_{1d} = \sqrt{P_{1T}} b_{11d} \mathbf{w}_{1r} + \sqrt{P_{2T}} b_{21d} \mathbf{w}_{2rn} + \mathbf{n}_{1d} \\ \mathbf{y}_{1s} = \sqrt{P_{1T}} b_{11s} \mathbf{w}_{1r} + \sqrt{P_{2T}} b_{21s} \mathbf{w}_{2rn} + \mathbf{n}_{1s} \end{cases} \quad (37)$$

$$H_0 : \begin{cases} \mathbf{y}_{2d} = \sqrt{P_{2T}} b_{22d} \mathbf{w}_{2r} + \sqrt{P_{1T}} b_{12d} \mathbf{w}_{1rm} + \mathbf{n}_{2d} \\ \mathbf{y}_{2s} = \mathbf{n}_{2s} \end{cases} \quad (38)$$

$$H_1 : \begin{cases} \mathbf{y}_{2d} = \sqrt{P_{1T}} b_{22d} \mathbf{w}_{2r} + \sqrt{P_{1T}} b_{12d} \mathbf{w}_{1rm} + \mathbf{n}_{2d} \\ \mathbf{y}_{2s} = \sqrt{P_{2T}} b_{22s} \mathbf{w}_{2r} + \sqrt{P_{1T}} b_{12s} \mathbf{w}_{1rm} + \mathbf{n}_{2s} \end{cases} \quad (39)$$

where $\|\mathbf{w}_{1r}\| = \|\mathbf{n}_{1d}\| = \|\mathbf{n}_{1s}\| = L_1$, $\|\mathbf{w}_{2r}\| = \|\mathbf{n}_{2d}\| = \|\mathbf{n}_{2s}\| = L_2$, $\|\mathbf{w}_{1rm}\| = \|\mathbf{w}_{2rn}\| = (1 - K_1 - K_2)$, $\|\cdot\|$ represent the length of the vector. The detection probabilities are

$$DP_1 \approx \mathcal{Q}_1 \left(\sqrt{2P_{1T} \gamma_{11s} \mathbf{w}_{1r}^H \mathbf{w}_{1r} + 2P_{2T} \gamma_{21s} \mathbf{w}_{2rn}^H \mathbf{w}_{2rn}}, b \right) \quad (40)$$

$$= \mathcal{Q}_1 \left(\sqrt{2P_{1T} \gamma_{11s} L_1 + 2P_{2T} \gamma_{21s} (L_2 - K_1)}, b \right)$$

$$DP_2 \approx \mathcal{Q}_1 \left(\sqrt{2P_{2T} \gamma_{22s} \mathbf{w}_{2r}^H \mathbf{w}_{2r} + 2P_{1T} \gamma_{12s} \mathbf{w}_{1rm}^H \mathbf{w}_{1rm}}, b \right) \quad (41)$$

$$= \mathcal{Q}_1 \left(\sqrt{2P_{1T} \gamma_{12s} (L_1 - K_2) + 2P_{2T} \gamma_{22s} L_2}, b \right)$$

It can be seen that, when the sensing times overlap, the two users can use each other's signals to increase the detection probabilities. This is a form of collaborative sensing.

3 | PERFORMANCE TRADEOFF AND OPTIMIZATION

Before the optimization problems are formulated, define $\alpha_1 = \frac{T_{1c}}{T}$ and $\alpha_2 = \frac{T_{2c}}{T}$ as the time allocation coefficients for user-1 and user-2, respectively. Thus, $T_{1c} = \alpha_1 T$, $T_{2c} = \alpha_2 T$, $T_{1r} = (1 - \alpha_1)T$ and $T_{2r} = (1 - \alpha_2)T$. Consequently, $L_1 = [\alpha_1 N]$, $K_1 = [(1 - \alpha_1)N]$, $L_2 = [\alpha_2 N]$, and $K_2 = [(1 - \alpha_2)N]$, with $0 \leq \alpha_1, \alpha_2 \leq 1$, where $[\cdot]$ is the rounding function.

3.1 | CS-CS

Assume that both users have the same transmission power and symmetric channels. This represents the scenario for two independent users. Using α_1 and α_2 , when $\alpha_1 > \alpha_2$, the information rates, the sum rate and the probabilities of detection in the CS-CS strategy can be rewritten as

$$C_1 = \alpha_2 T \log_2 \left(1 + \frac{P_T \gamma_c}{P_T \gamma_\Delta + 1} \right) + (\alpha_1 - \alpha_2) T_s \log_2 (1 + P_T \gamma_c) \quad (42)$$

$$C_2 = \alpha_2 T \log_2 \left(1 + \frac{P_T \gamma_c}{P_T \gamma_\Delta + 1} \right) \quad (43)$$

$$C = 2\alpha_2 T \log_2 \left(1 + \frac{P_T \gamma_c}{P_T \gamma_\Delta + 1} \right) + (\alpha_1 - \alpha_2) T \log_2 (1 + P_T \gamma_c) \quad (44)$$

$$DP : \begin{cases} DP_1 = \mathcal{Q}_1 \left(\sqrt{2(1 - \alpha_1) P_T (\gamma_s + \gamma_\Delta) N}, b \right) \\ DP_2 = \mathcal{Q}_1 \left(\sqrt{2P_T [(1 - \alpha_1) \gamma_s + (1 - \alpha_2) \gamma_\Delta] N}, b \right) \end{cases} \quad (45)$$

and when $\alpha_1 < \alpha_2$, the information rates, the sum rate, and the probabilities of detection can be rewritten as

$$C_1 = \alpha_1 T \log_2 \left(1 + \frac{P_T \gamma_c}{P_T \gamma_\Delta + 1} \right) \quad (46)$$

$$C_2 = \alpha_1 T \log_2 \left(1 + \frac{P_T \gamma_c}{P_T \gamma_\Delta + 1} \right) + (\alpha_2 - \alpha_1) T_s \log_2 (1 + P_T \gamma_c) \quad (47)$$

$$C = 2\alpha_1 T \log_2 \left(1 + \frac{P_T \gamma_c}{P_T \gamma_\Delta + 1} \right) + (\alpha_2 - \alpha_1) T \log_2 (1 + P_T \gamma_c) \quad (48)$$

$$DP : \begin{cases} DP_1 = \mathcal{Q}_1\left(\sqrt{2P_T[(1-\alpha_1)\gamma_s + (1-\alpha_2)\gamma_\Lambda]N}, b\right) \\ DP_2 = \mathcal{Q}_1\left(\sqrt{2(1-\alpha_2)P_T(\gamma_s + \gamma_\Lambda)N}, b\right) \end{cases} \quad (49)$$

where $P_T = P_{1T} = P_{2T}$. Also, $\gamma_c = \gamma_{11c} = \gamma_{22c}$, $\gamma_\Delta = \gamma_{12c} = \gamma_{21c}$, $\gamma_s = \gamma_{11s} = \gamma_{22s}$, $\gamma_\Lambda = \gamma_{12s} = \gamma_{21s}$ are the SNR of the communications channel, the communications interference channel, the sensing surveillance channel and the sensing cross-channel, respectively.

In the subsequent analysis, we will determine the optimal values of α_1 and α_2 which optimize sensing, communications, or both performances. The first optimization problem is formulated as

$$P_1 : \max_{\alpha_1, \alpha_2} \{\overline{DP}\}, \quad (50)$$

$$C_1 \geq C_m, C_2 \geq C_m, \quad \text{s.t.} \quad (51)$$

$$0 \leq \alpha_1, \alpha_2 \leq 1 \quad (52)$$

where C_m is the minimum communications rate for each user, $\overline{DP} = \frac{1}{2}(DP_1 + DP_2)$ is the average detection probability with DP_1 and DP_2 given by Equations (45) and (49) and C_1, C_2 are given by Equations (42)–(48). For applications prioritizing sensing over communications, this optimization aims to maximize the probability of detection while ensuring a minimum communication rate for each user.

The second optimization problem is given by

$$P_2 : \max_{\alpha_1, \alpha_2} \{C\}, \quad (53)$$

$$DP_1 \geq P_m, DP_2 \geq P_m, \quad \text{s.t.} \quad (54)$$

$$0 \leq \alpha_1, \alpha_2 \leq 1 \quad (55)$$

where P_m is the minimum detection probability for sensing. This optimization is for applications where the communications function is of more importance than the sensing function.

When both sensing and communications hold equal importance, or when neither has any constraints, the third optimization problem is

$$P_3 : \max_{\alpha_1, \alpha_2} \{U\}, \quad \text{s.t.} \quad (56)$$

$$0 \leq \alpha_1, \alpha_2 \leq 1 \quad (57)$$

where the unified metric U is the measure of performance trade-off between sensing and communications, which is defined as

$$U = \epsilon \overline{DP} + (1 - \epsilon) \frac{C}{C_{\max}}, \quad (58)$$

$0 < \epsilon < 1$ is the trade-off coefficient and it indicates the importance of sensing in the Pareto optimization problem [21]. In

Equation (58), C_{\max} is used to normalize the information rate so that both the probability of detection and the normalized information rate are between 0 and 1 for optimization. Next, we will solve these optimization problems.

For P_1 , when $\alpha_1 \geq \alpha_2$, $C_1 > C_2$ and when $\alpha_2 > \alpha_1$, $C_2 > C_1$. Thus, to satisfy the constraints in Equation (51)

$$\begin{cases} C_2 = \alpha_2 T \log_2 \left(1 + \frac{P_T \gamma_c}{P_T \gamma_\Delta + 1} \right) > C_m, \alpha_1 \geq \alpha_2 \\ C_1 = \alpha_1 T \log_2 \left(1 + \frac{P_T \gamma_c}{P_T \gamma_\Delta + 1} \right) > C_m, \alpha_1 < \alpha_2 \end{cases} \quad (59)$$

From Equation (59), one has

$$\begin{cases} 1 \geq \alpha_1 \geq \frac{C_m}{T \log_2 \left(1 + \frac{P_T \gamma_c}{P_T \gamma_\Delta + 1} \right)} \\ 1 \geq \alpha_2 \geq \frac{C_m}{T \log_2 \left(1 + \frac{P_T \gamma_c}{P_T \gamma_\Delta + 1} \right)} \end{cases} \quad (60)$$

where $C_m \leq T \log_2 \left(1 + \frac{P_T \gamma_c}{P_T \gamma_\Delta + 1} \right)$ must be satisfied. From Equations (45) and (49), the detection probabilities DP_1 and DP_2 increase monotonically as α_1 or α_2 decreases. Thus, the maximum \overline{DP} is achieved when α_1 and α_2 are the smallest. Then, the optimum values are

$$\begin{aligned} \alpha_{1\text{opt}} = \alpha_{2\text{opt}} = \alpha_{\text{opt}} \\ = \begin{cases} \frac{C_m}{T \log_2 \left(1 + \frac{P_T \gamma_c}{P_T \gamma_\Delta + 1} \right)}, & C_m \leq T \log_2 \left(1 + \frac{P_T \gamma_c}{P_T \gamma_\Delta + 1} \right) \\ \text{none}, & C_m > T \log_2 \left(1 + \frac{P_T \gamma_c}{P_T \gamma_\Delta + 1} \right) \end{cases} \end{aligned} \quad (61)$$

and

$$\begin{aligned} \overline{DP}_{\max} = \frac{1}{2} \left[\mathcal{Q}_1 \left(\sqrt{2(1 - \alpha_{\text{opt}})P_T(\gamma_s + \gamma_\Lambda)N}, b \right) \right. \\ \left. + \mathcal{Q}_1 \left(\sqrt{2P_T(1 - \alpha_{\text{opt}})(\gamma_s + \gamma_\Lambda)N}, b \right) \right] \end{aligned} \quad (62)$$

respectively.

For P_2 in Equation (53), when $\alpha_1 > \alpha_2$, $DP_2 \geq DP_1$ and when $\alpha_2 > \alpha_1$, $DP_1 > DP_2$ so that to satisfy the constraints in Equation (55)

$$\begin{cases} \mathcal{Q}_1 \left(\sqrt{2(1 - \alpha_1)P_T(\gamma_s + \gamma_\Lambda)N}, b \right) > P_m, \alpha_1 \geq \alpha_2 \\ \mathcal{Q}_1 \left(\sqrt{2(1 - \alpha_2)P_T(\gamma_s + \gamma_\Lambda)N}, b \right) > P_m, \alpha_2 < \alpha_1. \end{cases} \quad (63)$$

Since the Marcum Q function is monotonic, from Equation (63), one has

$$\begin{cases} 0 \leq \alpha_1 \leq 1 - \frac{[\mathcal{Q}_1^{-1}(P_m, b)]^2}{2P_T N(r_s + r_\Lambda)} \\ 0 \leq \alpha_2 \leq 1 - \frac{[\mathcal{Q}_1^{-1}(P_m, b)]^2}{2P_T N(r_s + r_\Lambda)} \end{cases} \quad (64)$$

where $\mathcal{Q}_1^{-1}(\cdot, \cdot)$ is the inverse function of $\mathcal{Q}_1(\cdot, \cdot)$ and $[\mathcal{Q}_1^{-1}(P_m, b)]^2 \leq 2P_T N(r_s + r_\Lambda)$ must be satisfied. The partial derivative of C with respect to α_2 is derived as

$$\frac{\partial C}{\partial \alpha_2} = 2T \log_2 \left(1 + \frac{P_T \gamma_\epsilon}{P_T \gamma_\Delta + 1} \right) - T \log_2 (1 + P_T \gamma_\epsilon). \quad (65)$$

When $P_T \gamma_\epsilon \geq P_T^2 \gamma_\Delta^2 - 1$, $\frac{\partial C}{\partial \alpha_2} \geq 0$ always holds. The same holds when $\alpha_1 < \alpha_2$. Thus, from Equations (64) and (65), the optimum values are

$$\begin{aligned} \alpha_{1\text{opt}} &= \alpha_{2\text{opt}} = \alpha_{\text{opt}} \\ &= \begin{cases} 1 - \frac{[\mathcal{Q}_1^{-1}(P_m, b)]^2}{2P_T N(r_s + r_\Lambda)}, & [\mathcal{Q}_1^{-1}(P_m, b)]^2 \leq 2P_T N(r_s + r_\Lambda) \\ \text{none}, & [\mathcal{Q}_1^{-1}(P_m, b)]^2 > 2P_T N(r_s + r_\Lambda) \end{cases} \end{aligned} \quad (66)$$

and

$$C_{\max} = 2\alpha_{\text{opt}} T \log_2 \left(1 + \frac{P_T \gamma_\epsilon}{P_T \gamma_\Delta + 1} \right) \quad (67)$$

For P_3 in Equation (58), there are no constraints on the probabilities of detection or the information rates so that one can simply take the first-order partial derivatives of U with respect to α_1 and α_2 and setting them to zero to give $\frac{\partial \overline{DP}}{\partial \alpha_1} + \frac{(1-\epsilon)\partial C}{C_{\max} \partial \alpha_1} = 0$ and $\frac{\partial \overline{DP}}{\partial \alpha_2} + \frac{(1-\epsilon)\partial C}{C_{\max} \partial \alpha_2} = 0$. There is no closed-form expression for the optimum values but these are nonlinear equations with only one variable, which can be easily solved by using mathematical software, such as MATLAB.

3.2 | CS-SC

Similarly, when $\alpha_1 + \alpha_2 > 1$, the information rates, the sum rate, and the probabilities of detection can be rewritten as

$$\begin{aligned} C_1 &= \alpha_1 T_s \log_2 (1 + P_T \gamma_\epsilon) \\ &+ (\alpha_1 + \alpha_2 - 1) T_s \log_2 \left(1 + \frac{P_T \gamma_\epsilon}{P_T \gamma_\Delta + 1} \right) \end{aligned} \quad (68)$$

$$\begin{aligned} C_2 &= \alpha_2 T_s \log_2 (1 + P_T \gamma_\epsilon) \\ &+ (\alpha_1 + \alpha_2 - 1) T_s \log_2 \left(1 + \frac{P_T \gamma_\epsilon}{P_T \gamma_\Delta + 1} \right) \end{aligned} \quad (69)$$

$$\begin{aligned} C &= (\alpha_1 + \alpha_2) T_s \log_2 (1 + P_T \gamma_\epsilon) \\ &+ 2(\alpha_1 + \alpha_2 - 1) T_s \log_2 \left(1 + \frac{P_T \gamma_\epsilon}{P_T \gamma_\Delta + 1} \right) \end{aligned} \quad (70)$$

$$DP : \begin{cases} DP_1 = \mathcal{Q}_1 \left(\sqrt{2(1 - \alpha_1) P_T \gamma_s N}, b \right) \\ DP_2 = \mathcal{Q}_1 \left(\sqrt{2(1 - \alpha_2) P_T \gamma_s N}, b \right). \end{cases} \quad (71)$$

and when $\alpha_1 + \alpha_2 < 1$, the information rates, the sum rate, and the probabilities of detection can be rewritten as

$$C_1 = \alpha_1 T_s \log_2 (1 + P_T \gamma_\epsilon) \quad (72)$$

$$C_2 = \alpha_2 T_s \log_2 (1 + P_T \gamma_\epsilon) \quad (73)$$

$$C = (\alpha_1 + \alpha_2) T_s \log_2 (1 + P_T \gamma_\epsilon) \quad (74)$$

DP :

$$\begin{cases} DP_1 = \mathcal{Q}_1 \left(\sqrt{2[(1 - \alpha_1)\gamma_s + (1 - \alpha_1 - \alpha_2)\gamma_\Lambda] P_T N}, b \right) \\ DP_2 = \mathcal{Q}_1 \left(\sqrt{2[(1 - \alpha_1 - \alpha_2)\gamma_\Lambda + (1 - \alpha_2)\gamma_s] P_T N}, b \right). \end{cases} \quad (75)$$

The optimization problems are similar to these in P_1, P_2, P_3 , but in this case \overline{DP} is given by Equation (71) or (75), C is given by Equations (70)–(74), and other symbols are defined as before. These optimization problems can be solved in the following.

In the CS-SC strategy, the expressions of C and \overline{DP} are asymmetric in the two cases of $\alpha_1 + \alpha_2 \geq 1$ and $\alpha_1 + \alpha_2 < 1$. When $P_T \gamma_\epsilon \geq P_T^2 \gamma_\Delta^2 - 1$, the communication functions of two users overlap but the sum rate will still increase. Under this condition, C increases when α_1 or α_2 increases, and \overline{DP} decreases with α_1 or α_2 increases.

For P_1 , when $\alpha_1 + \alpha_2 \geq 1$, one has

$$\begin{cases} C_1 = (\alpha_1 + \alpha_2 - 1) T_s \log_2 \left(1 + \frac{P_T \gamma_\epsilon}{P_T \gamma_\Delta + 1} \right) \\ \alpha_1 T_s \log_2 (1 + P_T \gamma_\epsilon) > C_m, \alpha_1 \leq \alpha_2 \\ C_2 = (\alpha_1 + \alpha_2 - 1) T_s \log_2 \left(1 + \frac{P_T \gamma_\epsilon}{P_T \gamma_\Delta + 1} \right) \\ \alpha_2 T_s \log_2 (1 + P_T \gamma_\epsilon) > C_m, \alpha_1 > \alpha_2, \end{cases} \quad (76)$$

and when $\alpha_1 + \alpha_2 < 1$, one has

$$\begin{cases} C_1 = \alpha_1 T_s \log_2 (1 + P_T \gamma_\epsilon) > C_m, \alpha_1 \leq \alpha_2 \\ C_2 = \alpha_2 T_s \log_2 (1 + P_T \gamma_\epsilon) > C_m, \alpha_1 > \alpha_2. \end{cases} \quad (77)$$

Using Equations (76) and (77), one has

$$\begin{cases} 0 \leq \alpha_1 \leq \frac{C_m}{A}, C_m \leq A \\ 0 \leq \alpha_2 \leq \frac{C_m}{A}, C_m \leq A \\ 0 \leq \alpha_1 \leq \frac{C_m + B}{2B + A}, A < C_m \leq A + B \\ 0 \leq \alpha_2 \leq \frac{C_m + B}{2B + A}, A < C_m \leq A + B \end{cases} \quad (78)$$

where $A = T_s \log_2(1 + P_T \gamma_c)$ and $B = T_s \log_2(1 + \frac{P_T \gamma_c}{P_T \gamma_\Delta + 1})$. It can be seen from Equations (71) and (75) that \overline{DP} monotonically increases when α_1 or α_2 decreases. Thus, the maximum \overline{DP} is achieved when α_1 or α_2 is smallest, so the optimum values are

$$\begin{aligned} \alpha_{1\text{opt}} &= \alpha_{2\text{opt}} = \alpha_{\text{opt}} \\ &= \begin{cases} \frac{C_m}{A}, C_m \leq A \\ \frac{C_m + B}{2B + A}, A < C_m \leq A + B \\ \text{none}, C_m > A + B \end{cases} \end{aligned} \quad (79)$$

and

$$\overline{DP}_{\text{max}} = \begin{cases} \mathcal{Q}_1(\sqrt{2(1 - \alpha_1)P_T \gamma_s N}, b), C_m \leq A \\ \mathcal{Q}_1(\sqrt{2[(1 - 2\alpha_{\text{opt}})\gamma_\Lambda + (1 - \alpha_{\text{opt}})\gamma_s]P_T N}, b), \\ A < C_m \leq A + B \\ \text{none}, C_m > A + B \end{cases} \quad (80)$$

For P_2 , when $\alpha_1 + \alpha_2 \geq 1$, one has

$$\begin{cases} \mathcal{Q}_1(\sqrt{2(1 - \alpha_1)P_T \gamma_s N}, b) > P_m, \alpha_1 \geq \alpha_2 \\ \mathcal{Q}_1(\sqrt{2(1 - \alpha_2)P_T \gamma_s N}, b) > P_m, \alpha_2 < \alpha_1, \end{cases} \quad (81)$$

and when $\alpha_1 + \alpha_2 < 1$, one has

$$\begin{cases} \mathcal{Q}_1(\sqrt{2[(1 - \alpha_1)\gamma_s + 2(1 - \alpha_1 - \alpha_2)\gamma_\Lambda]P_T N}, b) > P_m, \alpha_1 \geq \alpha_2 \\ \mathcal{Q}_1(\sqrt{2[(1 - \alpha_1 - \alpha_2)\gamma_\Lambda + (1 - \alpha_2)\gamma_s]P_T N}, b) > P_m, \alpha_2 < \alpha_1. \end{cases} \quad (82)$$

Since the Marcum \mathcal{Q} function is monotonic, from Equations (81) and (82), one has

$$\begin{cases} 0 \leq \alpha_1, \alpha_2 \leq 1 - \frac{D}{E_1}, D \leq E_1 \\ 0 \leq \alpha_1, \alpha_2 \leq 1 - \frac{D + E_2}{E_1 + 2E_2}, E_1 < D \leq E_1 + E_2 \end{cases} \quad (83)$$

where $\mathcal{Q}_1^{-1}(\cdot, \cdot)$ is the inverse function of $\mathcal{Q}_1(\cdot, \cdot)$, and $D = [\mathcal{Q}_1^{-1}(P_m, b)]^2$, $E_1 = 2PN\gamma_s$ and $E_2 = 2PN\gamma_\Lambda$. One sees from

Equations (70) and (74) that C increases when α_1 or α_2 increase. Thus, the maximized C_{max} is achieved when α_1 or α_2 is the largest, so the optimum values are

$$\begin{aligned} \alpha_{1\text{opt}} &= \alpha_{2\text{opt}} = \alpha_{\text{opt}} \\ &= \begin{cases} 1 - \frac{D}{E_1}, D \leq E_1 \\ 1 - \frac{D + E_2}{E_1 + 2E_2}, E_1 < D \leq E_1 + E_2 \\ \text{none}, D > E_1 + E_2 \end{cases} \end{aligned} \quad (84)$$

and

$$C_{\text{max}} = \begin{cases} 2(2\alpha_{\text{opt}} - 1)T_s \log_2\left(1 + \frac{P_T \gamma_c}{P_T \gamma_\Delta + 1}\right) \\ + 2\alpha_{\text{opt}}T_s \log_2(1 + P_T \gamma_c), D \leq E_1 \\ (\alpha_1 + \alpha_2)T_s \log_2(1 + P_T \gamma_c), E_1 < D \leq E_1 + E_2 \\ \text{none}, D > E_1 + E_2 \end{cases} \quad (85)$$

For P_3 , taking the first-order partial derivatives of U with respect to α_1 and α_2 and setting them to zero, one has $\frac{\epsilon \partial \overline{DP}}{\partial \alpha_1} + \frac{(1 - \epsilon) \partial C}{C_{\text{max}} \partial \alpha_1} = 0$ and $\frac{\epsilon \partial \overline{DP}}{\partial \alpha_2} + \frac{(1 - \epsilon) \partial C}{C_{\text{max}} \partial \alpha_2} = 0$. Again, there is no closed-form expression but they can be solved using MATLAB.

4 | NUMERICAL RESULTS AND DISCUSSION

In this section, numerical examples are presented to show the performances of the dual-user JSAC systems. In the examples, the parameters are set as: $P_T = 1$, $T = 10$, $T_s = 0.5$, $\epsilon = 0.5$, $EA = 0.01$, $N = 20$. The examination focuses on the effects of the time allocation parameters α_1 and α_2 on the system performance. The performances of sensing and communications are measured by the average detection probability \overline{DP} and the sum rate C , respectively.

Figures 2–4 show the system performances using the CS–CS strategy. Figure 2 shows how the average detection probability \overline{DP} changes with different time allocation parameters α_1 and α_2 with communications constraints as P_1 in Equation (50). Several observations can be made. First, \overline{DP} starts from zero in all cases. This is because when α_1 and α_2 are too small, the communications rates C_1 or C_2 do not reach the minimum communications rate C_m and hence, both DP_1 and DP_2 are set to 0. Second, \overline{DP} starts from 1 when the minimum rate is met but then decreases, when α_1 or α_2 increase. This is because the partial derivatives of DP_1 and DP_2 with respect to α_1 or α_2 are lower than zero from Equations (45) and (49). Third, similar observations can be made for both α_1 and α_2 . These observations also explain why \overline{DP} has turning points at 1. Note that the maximum \overline{DP} is obtained at 1 when α_1 and α_2 are between 0.6 and 0.7 in each sub-figure. This gives flexibility to the choice values of α_1 and α_2 .

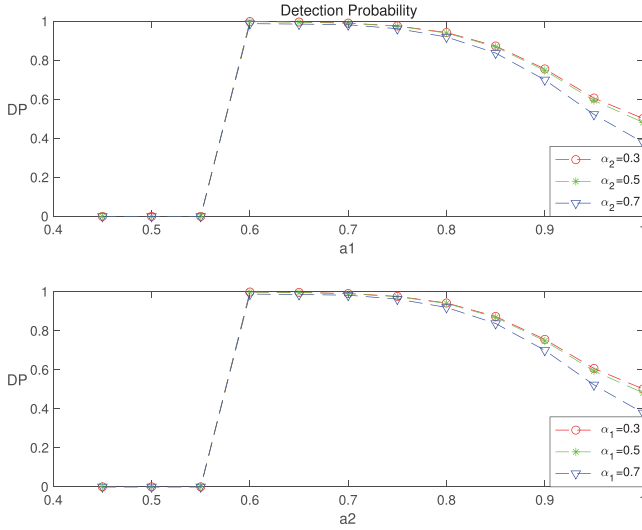


FIGURE 2 The average detection probability \overline{DP} versus α_1 and α_2 when $\delta = 0$ dB, $\gamma_s = 1$ dB for CS-CS.

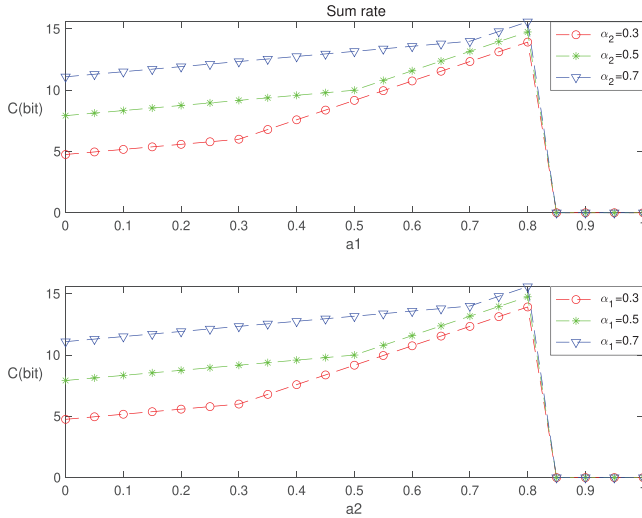


FIGURE 3 The sum rate C versus α_1 and α_2 when $\delta = 0$ dB, $\gamma_s = 1$ dB for CS-CS.

Figure 3 shows how the sum rate C changes with different time allocation parameters α_1 or α_2 with sensing constraints as P_2 in Equation (54). In order to consider the impact of interference between different users on the optimal performance of the system, we set $\delta = 0$ dB. First, C starts from a fixed value when $\alpha_1 = 0$ and $\alpha_2 = 0$ but ends with zero when α_1 and α_2 are large. When $\alpha_1 = 0$, α_2 takes three possible non-zero values: 0.3, 0.5, and 0.7. Thus, when $\alpha_1 = 0$ and there is no communications activity from user-1, user-2 still has communications activity and vice versa. Therefore, the sum rate exists when $\alpha_1 = 0$ or $\alpha_2 = 0$. When DP_1 or DP_2 cannot meet the minimum detection probability P_m , the sum rate C drops to zero. This was set by our experiment to show that the system cannot meet the optimization requirement in this case. The sum rate reaches the maximum value of 16, and then decreases to 0 when α_1 or α_2 increase from 0 to 1, because the partial derivatives of

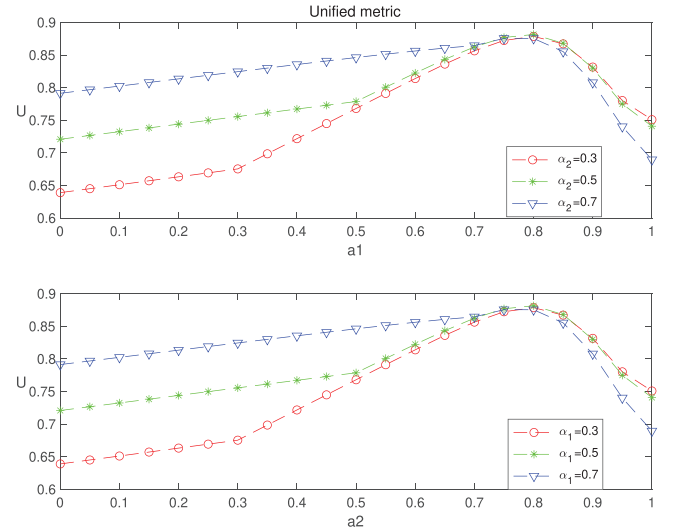


FIGURE 4 The unified metric U versus α_1 and α_2 when $\delta = 0$ dB, $\gamma_s = 1$ dB for CS-CS.

C with respect to α_1 or α_2 are larger than zero from Equations (44) and (48), but when α_1 or α_2 reach 0.85, DP_1 or DP_2 cannot meet the minimum detection probability P_m , so the sum rate C is set to 0 and the optimization is not possible in this case. This also explains why the curves in the figure have a turning point around 16, as the sum rate increases with α_1 and α_2 and then is set to zero. Note that the maximum C is obtained when α_1 and α_2 are 0.8 in each sub-figure. This is due to the symmetric channel settings used. It can be verified that the optimum values observed from the figures are the same as those calculated in Section 3. For example, in Figure 3, if $\alpha_1 = 0.7$, C reaches the maximum value of 15.585 when $\alpha_2 = 0.8$. Using Equation (67), this value is calculated as 16 when $\alpha_1 = \alpha_2 = 0.8$.

Figure 4 shows how the unified metric U changes with different time allocation parameters α_1 or α_2 as P_3 from Equation (56). The value of U is always between 0 and 1 and is never zero. This is because the normalization is completed with respect to C and no sensing or communications constraints are imposed. Also, they increase first and then decrease when α_1 or α_2 increase. This is because when α_1 or α_2 are small, the sum rate C keeps increasing when α_1 or α_2 increase, but the average detection probability \overline{DP} is almost unchanged so that U continues to increase. When α_1 or α_2 are large, the average detection probability \overline{DP} is significantly reduced, so U begins to decrease. These lead to a turning point around 0.85 in the figure. Note that the maximum U is obtained when α_1 and α_2 are 0.8 in each sub-figure.

Figures 5–7 show the system performances for the CS-SC strategy. Figure 5 shows how the average detection probability \overline{DP} changes with α_1 or α_2 . The \overline{DP} still increases from 0 to 1 and then decreases again, when α_1 or α_2 increase. This is also because when α_1 or α_2 are small the communications rates C_1 or C_2 don't reach the minimum communications rate C_m and hence, both DP_1 and DP_2 are set to 0. When α_1 or α_2 increase, the communications rates C_1 or C_2 can meet the minimum communications rate C_m and \overline{DP} is a fixed value.

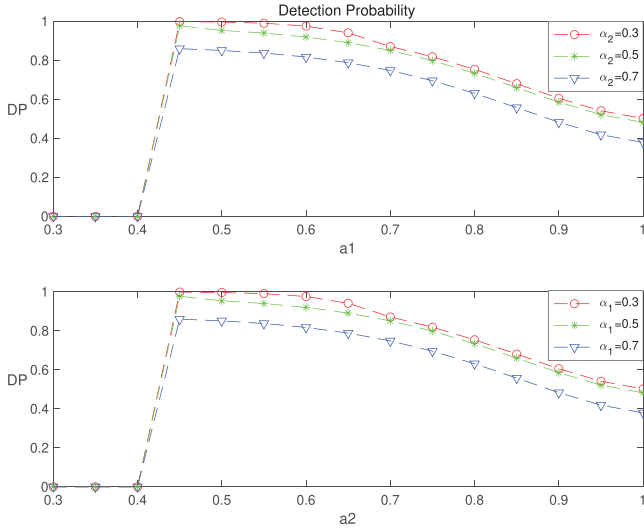


FIGURE 5 The average detection probability \overline{DP} versus α_1 and α_2 when $\delta = 0$ dB, $\gamma_s = 1$ dB for CS-SC.

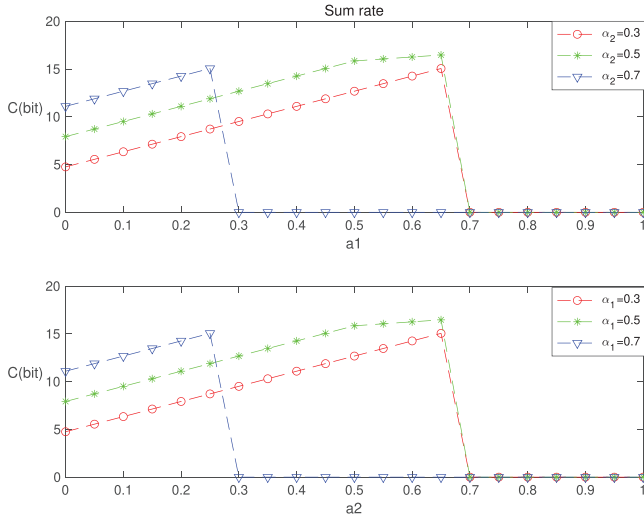


FIGURE 6 The sum rate C versus α_1 and α_2 when $\delta = 0$ dB, $\gamma_s = 1$ dB for CS-SC.

The partial derivatives of \overline{DP} with respect to α_1 or α_2 are smaller than zero, so \overline{DP} decreases when α_1 or α_2 increase. When $\alpha_1 = 0.7$ or $\alpha_2 = 0.7$, \overline{DP} cannot reach 1 anymore. This is because when α_1 or α_2 are large, little time is allocated to sensing. In addition, when sensing and communications of two users are performed in different orders, the user-1 or user-2 cannot use each other's sensing signals to increase the detection probability, so DP_1 or DP_2 cannot reach 1. Note that the maximum \overline{DP} is still obtained when α_1 and α_2 are around 0.45 in each sub-figure.

Figure 6 shows C versus α_1 or α_2 . Here, C increases from a fixed value to the maximum value and then decreases to 0 when α_1 or α_2 increase from 0 to 1, similar to Figure 3. Also, the sum rate C at $\alpha_2 = 0.7$ or $\alpha_1 = 0.7$ decrease to 0 when α_1 or α_2 is 0.3, respectively. Additionally, when sensing and communica-

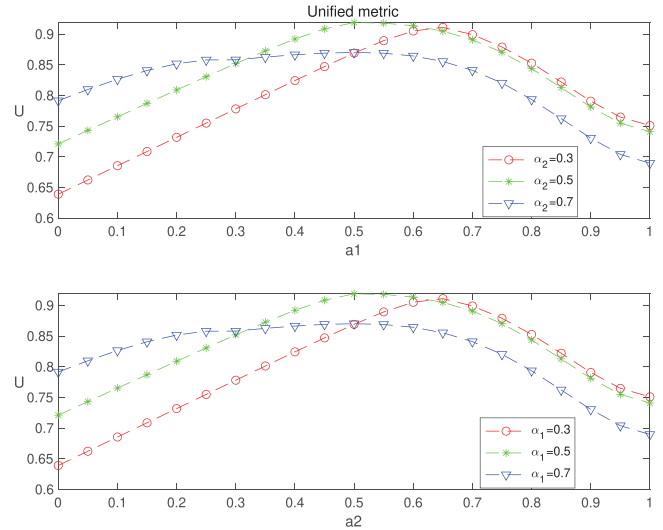


FIGURE 7 The unified metric U versus α_1 and α_2 when $\delta = 0$ dB, $\gamma_s = 1$ dB for CS-SC strategy.

tions of two users are performed in different orders, user-1 or user-2 cannot use each other's sensing signals to increase the detection probability, so DP_1 or DP_2 cannot reach the minimum detection probability P_m and C is set to zero. Moreover, C increases faster than that in Figure 3. This is because there is no interference between communications signals of two user when they perform sensing and communications in different orders.

Figure 7 shows how the unified metric U changes with α_1 or α_2 . Different from Figure 4, there are intersection points between different curves. This means the same performance tradeoff can be achieved under different combinations of α_1 and α_2 . Also, different curves reach their maximum values at different times. This is because the sensing and communications no longer have the same maximum values when α_1 or α_2 change. From the previous figures, one sees that allocating more time to communications in general improves communications rate but degrades sensing performance, and vice versa. However, this also depends on the JSAC order, as changing the order can reduce interference. Also, our work does not consider power allocation but this can affect the tradeoff between sensing and communications as well, if the total power is fixed. Similarly, \overline{DP} in Figure 5, C in Figure 6 and U in Figure 7 have extreme points for the same reason as those in Figures 2, 3, and 4, respectively.

Figures 8 and 9 compare the maximum average detection probability and sum rate for the CS-CS and CS-SC strategies with two benchmarks. Benchmark 1 and Benchmark 2 both allocate the time equally between sensing and communications for CS-CS and CS-SC, respectively, or $\alpha_1 = 0.5$ and $\alpha_2 = 0.5$.

In Figure 8, several observations can be made. First, DP_{\max} increases from 0 to 1 when γ_s increase from -10 to 10 dB. This is because when the SNR of the sensing channels increases, the received signals at the sensing receivers are enhanced. Second, DP_{\max} of CS-SC strategy is always higher than that of CS-CS strategy. This is because the interference between

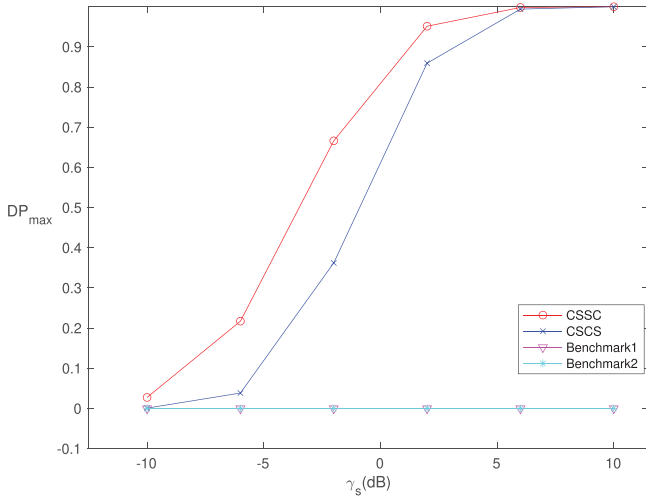


FIGURE 8 Comparison of the maximum \overline{DP} for the CS-CS and CS-SC strategies.

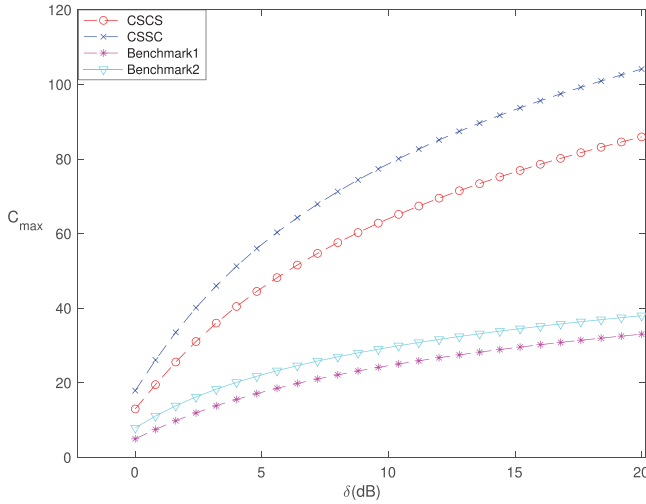


FIGURE 9 Comparison of the maximum sum rate C for the CS-CS and CS-SC strategies.

communication signals is serious under the CS-CS strategy. This reduces the sum rate of CS-CS. Consequently, it is harder to meet the constraints in Equation (51) and degrade the detection performance. For the CS-SC scheme, since users perform communications and sensing in the opposite order and sensing and communications operate at different frequencies without interference, the interference between communications signals is smaller and the sum rate is larger. Since the two benchmarks cannot meet the communications requirements, their DP_{\max} is always 0.

This is revealed in Figure 9, which compares the maximum sum rate for the CS-CS and CS-SC strategies. First, C_{\max} always increases when δ increases from 0 to 20 dB. This is because, when the SINR of the communications channels increases, the received signals at the communications receivers are enhanced.

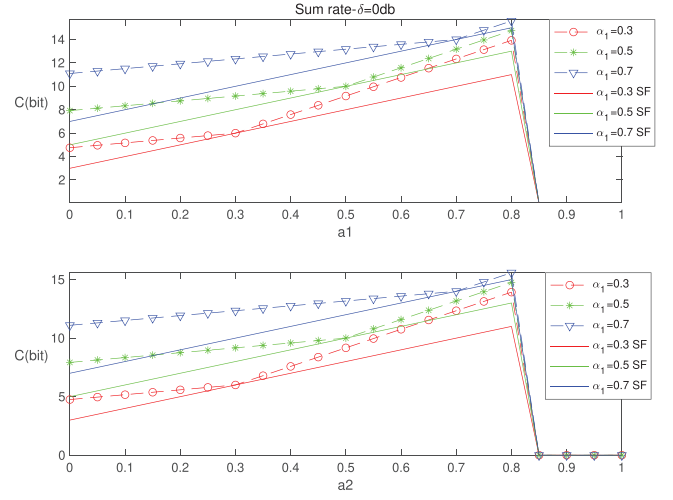


FIGURE 10 Sum rate comparison of communications and sensing with the same frequency and different frequency for the CS-CS strategy.

Second, C_{\max} of CS-SC strategy is higher than that of CS-CS strategy. Again, this is because of less interference between communications signals in the CS-SC strategy. Both CS-CS and CS-SC strategies have better performance than the two benchmarks. From the comparison, better system performance can be achieved by choosing optimal time allocation coefficients. Both sensing and communications performances under the CS-SC strategy are better than those in the CS-CS strategy.

The above results have assumed different frequencies for sensing and communications. Figure 10 compares the sum rate for JSAC using the same frequency (SF) and that using different frequencies in the CS-CS strategy. One sees that higher sum rate can be achieved when JSAC uses different frequencies than that uses the same frequency. This agrees with intuition. However, our results quantify their difference. Moreover, the optimal values of time allocation are also shown in all cases. This is expected. For example, the optimum value for α_1 in the upper part of Figure 10 is the same as that for α_2 in the lower part of Figure 10, as predicted by Equation (66). All the curves in Figure 10 for different values of α_1 or α_2 have the same optimum value of 0.8, as predicted by Equation (66) where α_{opt} does not depend on α_1 or α_2 . The optimum value in this case is 0.8, close to 1, which can also be calculated using $1 - \frac{[Q_1^{-1}(P_{m,b})]^2}{2P_T N(r_s + r_\Lambda)}$ in Equation (66). Note that these curves increase with α_1 or α_2 and then decrease to zero to have extreme points at around 16, for the same reason as Figure 3.

Figure 11 compares the proposed scheme with that in [21] for the unified metric U . One sees that the proposed scheme always has a higher maximum U than that in [21], showing the advantage of the work. One also sees that the proposed scheme achieves the maximum U at $\alpha_1 = \alpha_2 = 0.8$, while the scheme in [21] achieves the maximum U at $\alpha_1 = \alpha_2 = 0.95$. Note that the value of U first increases and then decreases with α_1 or α_2 to have extreme points at around 0.85 or 0.79, for the same reason as Figure 4.

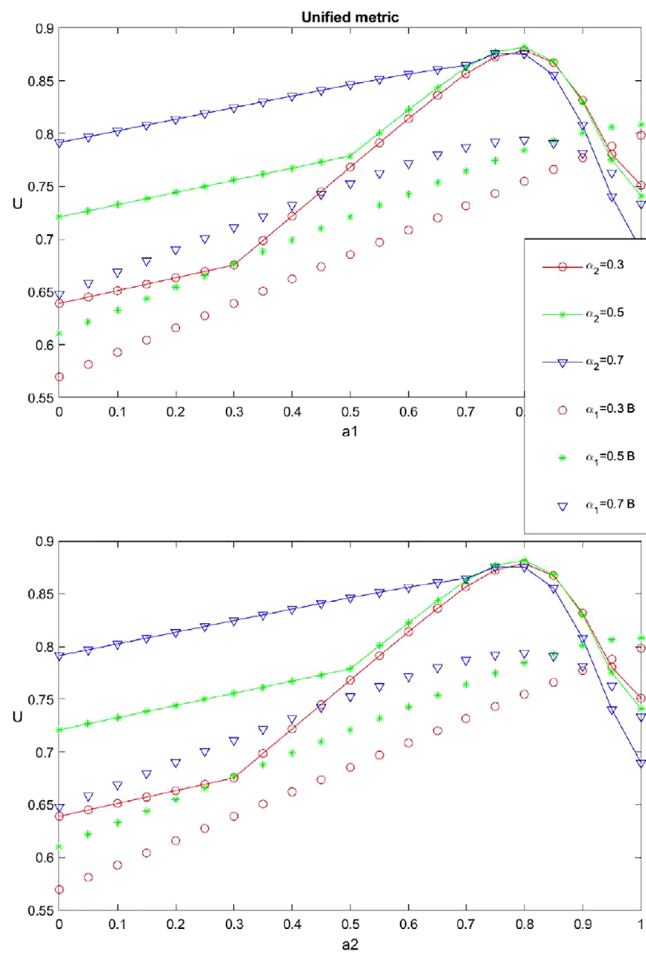


FIGURE 11 Comparison of the proposed scheme with [21].

5 | CONCLUSION

In this work, a dual-user JSAC system based on time division has been studied using bi-static settings, when two users perform sensing and communications in the same order or in the opposite order. For both schemes, three optimization strategies have been investigated. By comparing the optimal performances of the two schemes, numerical results have demonstrated that the CS-SC scheme provides the best performance. Note that this work assumes two users. The complexity of the problem increases exponentially with the number of users and thus, arbitrary numbers of users will be considered in future works.

AUTHOR CONTRIBUTIONS

Enhao Wang: Formal analysis; investigation; methodology; visualization; writing—original draft. **Yunfei Chen:** Conceptualization; methodology; supervision; writing—review and editing. **Aissa Ikhlef:** Writing—review and editing. **Hongjian Sun:** Writing—review and editing.

CONFLICT OF INTEREST STATEMENT

The authors declare no conflicts of interest.

DATA AVAILABILITY STATEMENT

The data that support the findings of this study are available from the corresponding author upon reasonable request.

ORCID

Enhao Wang  <https://orcid.org/0009-0001-6146-2474>

Yunfei Chen  <https://orcid.org/0000-0001-8083-1805>

Hongjian Sun  <https://orcid.org/0000-0001-8660-8081>

REFERENCES

- Wang, C.-X., Wang, J., Hu, S., Jiang, Z.H., Tao, J., Yan, F.: Key technologies in 6G terahertz wireless communication systems: a Survey. *IEEE Vehicular Technology Magazine* 16(4), 27–37 (2021). <https://doi.org/10.1109/MVT.2021.3116420>
- Paul, B., Chiriyath, A.R., Bliss, D.W.: Survey of RF communications and sensing convergence research. *IEEE Access* 5, 252–270 (2017)
- Fang, X., Feng, W., Chen, Y., Ge, N., Zhang, Y.: Joint communication and sensing toward 6G: models and potential of using MIMO. *IEEE Internet of Things J.* 10(5), 4093–4116 (2023). <https://doi.org/10.1109/JIOT.2022.3227215>
- Ahmadipour, M., Kobayashi, M., Wigger, M., Giuseppe, C.: An information-theoretic approach to joint sensing and communication. *IEEE Trans. Inf. Theory* 70, 1124–1146 (2024)
- Ghorbanzadeh, M., Vistosky, E., Moorut, P., Yang, W., Clancy, C.: Radar in-band interference effects on macrocell LTE uplink deployments in the US 3.5 GHz band. In: *Proceedings of the 2015 IEEE International Conference on Computing, Networking and Communications*, pp. 248–254. IEEE, Piscataway, NJ (2015)
- Raymond, S.-S., Abubakari, A., Jo, H.-S.: Coexistence of power-controlled cellular networks with rotating radar. *IEEE J. Sel. Areas Commun.* 34(10), 2605–2616 (2016). <https://doi.org/10.1109/JSAC.2016.2605978>
- Masarik, M.P., Subotic, N.S.: Cramer-Rao lower bounds for radar parameter estimation in noise plus structured interference. In: *Proceedings of the IEEE Radar Conference*, pp. 1–4. IEEE, Piscataway, NJ (2016)
- Grossi, E., Lops, M., Venturino, L.: Joint design of surveillance radar and MIMO communication in cluttered environments. *IEEE Trans. Signal Processing* 68, 1544–1557 (2020). <https://doi.org/10.1109/TSP.2020.2974708>
- Jiang, Z.-M., Zhang, P.-C., Huang, L., He, X., Zhang, J.-H., Rihan, M.: Transmit beam pattern optimization for automotive MIMO radar coexisted with communication in V2V networks. *Sensors* 20, 1100 (2020)
- Sodagari, S., Khawar, A., Clancy, T.C., McGwier, R.: A project based approach for radar and telecommunication systems coexistence. In: *Proceedings of the 2012 IEEE Global Communications Conference (GLOBECOM)*, pp. 1–5. IEEE, Piscataway, NJ (2012)
- Xiao, Z., Zeng, Y.: An overview on integrated localization and communication towards 6G. *Sci. China Inf. Sci.* 65, 131301 (2022)
- Brenner, T., Weiss, G., Klein, M., Kuschel, H.: Signals and data fusion in a deployable multiband passive-active radar (DMPAR). In: *IET International Conference on Radar Systems (Radar 2012)*, pp. 1–6. IEEE, Piscataway, NJ (2012)
- Griffiths, H.: Developments in bistatic and networked radar. In: *Proceedings of 2011 IEEE CIE International Conference on Radar*, pp. 10–13. IEEE, Piscataway, NJ (2011)
- Liu, F., et al.: Integrated sensing and communications: toward dual-functional wireless networks for 6G and beyond. *IEEE J. Sel. Areas Commun.* 40(6), 1728–1767 (2022). <https://doi.org/10.1109/JSAC.2022.3156632>
- Yao, Y., Miao, P., Chen, Z.: Cognitive waveform optimization for phase-modulation-based joint radar-communications system. *IEEE Access* 8, 33276–33288 (2020)
- Sturm, C., Wiesbeck, W.: Waveform design and signal processing aspects for fusion of wireless communications and radar sensing. *Proc. IEEE* 99, 1236–1259 (2011)

17. Cui, G., Liu, J., Li, H., Himed, B.: Signal detection with noisy reference for passive sensing. *Signal Process.* (108), 389–399 (2015)
18. Chen, Y., Wu, Y., Chen, N., Feng, W., Zhang, J.: New approximate distributions for the generalized likelihood ratio test detection in passive radar. *IEEE Signal Process. Lett.* 26, 685–689 (2019)
19. Liu, A., et al.: A survey on fundamental limits of integrated sensing and communication. *IEEE Commun. Surv. Tut.* 24(2), 994–1034 (2022). <https://doi.org/10.1109/COMST.2022.3149272>
20. Chalise, B.K., Amin, M.G., Himed, B.: Performance tradeoff in a unified passive radar and communications system. *IEEE Signal Process. Lett.* 24, 1275–1279 (2017)
21. Cao, N., Chen, Y., Gu, X., Feng, W.: Joint bi-static radar and communications designs for intelligent transportation. *IEEE Trans. Veh. Technol.* 69(11), 13060–13071 (2020)
22. Chen, Y., Gu, X.: Time allocation for integrated bi-static radar and communication systems. *IEEE Commun. Lett.* 25(3), 1033–1036 (2021)
23. Liu, P., Fei, Z., Wang, X., Zhang, J.A., Zheng, Z., Zhang, Q.: Securing multi-user uplink communications against mobile aerial eavesdropper via sensing. *IEEE Trans. Veh. Technol.* 72(7), 9608–9613 (2023)
24. Liao, Z., Liu, F.: Symbol-level precoding for integrated sensing and communications: a faster-than-Nyquist approach. *IEEE Commun. Lett.* 27(12), 3210–3214 (2023)
25. Ding, Z., Fan, P., Poor, H.V.: Impact of user pairing on 5G nonorthogonal multiple-access downlink transmissions. *IEEE Trans. Veh. Technol.* 65(8), 6010–6023 (2016)
26. Zhong, K., Hu, J., Pan, C.: Constant modulus MIMO radar waveform design via iterative optimization network method. *IEEE Trans. Instrum. Meas.* 72, 1–11 (2023)
27. Gradshteyn, I.S., Ryzhik, I.M.: *Table of Integrals, Series and Products*, 7th ed. Academic Press, London (2007)

How to cite this article: Wang, E., Chen, Y., Ikhlef, A., Sun, H.: Dual-user joint sensing and communications with time-divisioned bi-static radar. *IET Commun.* 1–14 (2024). <https://doi.org/10.1049/cmu2.12820>